Dielectric, electrical and infrared studies of gFe$_2$O$_3$ prepared by combustion method

VIJAY A HIREMATH[†] and A VENKATARAMAN*

Department of Chemistry, Gulbarga University, Gulbarga 585 106, India
[†]R.N.S. Institute of Technology, Channasandra, Bangalore 560 061, India

Abstract. This paper reports the electrical and spectroscopic investigation of the gamma ferrite synthesized through combustion route. The electrical study and dielectric behaviour showed a typical ferrite nature for the samples. The $g \rightarrow a$ transition is observed from the electrical conductivity data. Infrared spectral study showed the transition of a typical ferrite. The effect of the presence of a-impurities in gFe$_2$O$_3$ is also explained here.

Keywords. gFe$_2$O$_3$; combustion synthesis; dielectric behaviour; electrical conductivity; spectroscopic studies; chemical homogeneity.

1. Introduction

Iron oxides are important materials for many industrial applications such as pigments, magnetic materials, catalysts and sensors (Gulabshankar and Darshane 1991; Young *et al* 1996; Gopal Reddy *et al* 2000; Jung and Feldmann 2000; Aruna *et al* 2001). Much attention has been focused on magnetic recording media materials, due to the increase in need for high area density. Iron oxide mainly occurs in three different forms viz. FeO, Fe$_2$O$_3$ and Fe$_3$O$_4$. Fe$_2$O$_3$ has two crystallographic phases, a-Fe$_2$O$_3$ and gFe$_2$O$_3$, whereas gFe$_2$O$_3$ and Fe$_3$O$_4$ have the inverse spinel structure and are used for magnetic recording application. Oxidic spinels show interesting electrical, thermal, magnetic and catalytic properties. In these compounds, the properties are controlled by the nature of ions, their charge and the site distribution amongst tetrahedral and octahedral sites (Gulabshankar and Darshane 1991; Eberhard and Thomas 1998). gFe$_2$O$_3$ has inverse spinel structure and is represented as Fe^{+3}[Fe$^{+3}_{40/3}$ □$_{1/8}$] O$_{32}$, where □ represents the vacancy sites present in the lattice. The Fe^{+3} ions outside the square bracket represent tetrahedral position and the Fe^{+3} ions inside the square bracket represent the octahedral position. The structure is based around a face centred cubic array of oxygen atoms with the cations filling either the tetrahedral [A] or octahedral [B] interstices within this array. There are 16 (out of 32) occupied octahedral sites and 8 (out of 64) occupied tetrahedral sites in the unit cell gFe$_2$O$_3$. Electrical and magnetic properties of these ferrites are strongly dependent on the chemical composition, cation distribution and method of preparation in general and structure in particular (Murthy

and Sobhanadri 1976; Murthy 1990). The infrared spectrum is an important tool to probe various ordering phenomenon and this technique also gives information not only about the position of the ions in the crystal but also their vibrational modes in the crystal (Waldron 1955). The polycrystalline ferrites are very good dielectric materials. This may be possible because, in the process of preparation of ferrites, under slightly reduced conditions, the divalent iron formed in the body of the ferrite material leads to high conductivity grains. When such materials are cooled in an oxygen atmosphere, it is possible to form layers of very low conductivity over its constituent grains. Almost all the ferrites in the polycrystalline form have relatively high conductivity grains separated by low conductivity layers, so that they behave as a homogeneous dielectric material (Murthy 1990). Grain size effect and processing route in the synthesis of ferrites have found to have relationship on power loss, low eddy current losses and better magnetic properties. Small grain size has given rise to the low power loss and this is attributed to unique uniformity and higher chemical homogeneity and grain uniformity in Mn–Zn ferrites (Sale *et al* 1995). We have observed that as the particle size approach nano dimension in ferrites, the dielectric constant increases. The effect of particle morphology was also observed (Mallikarjun 2002; Mallikarjuna and Venkataraman 2003).

In this paper we report dielectric behaviour, temperature variation of d.c. electrical conductivity, and infrared spectroscopy of synthesized gFe$_2$O$_3$ sample, prepared from a-Fe$_2$O$_3$ using polyethylene glycol (PEG) as a fuel as reported. The effect of a-Fe$_2$O$_3$ impurities present in the gFe$_2$O$_3$ sample is also reported. The gFe$_2$O$_3 \rightarrow a$-Fe$_2$O$_3$ transition on the basis of temperature variation of electrical conductivity is also reported.

*Author for correspondence

2. Experimental

The detailed synthesis of γFe$_2$O$_3$ was reported earlier (Venkataraman *et al* 2001; Vijay and Venkataraman 2001), wherein, purified γFe$_2$O$_3$ was mixed with polyethylene glycol in a weight ratio of 1 : 2, 1 : 3, 1 : 4 and 1 : 5. Then, the mixture was heated to around 250°C in a silicon crucible. Polyethylene glycol melted and formed a dispersed phase with α-Fe$_2$O$_3$ at low temperature. The dispersed phase initially boiled and then immediately ignited, undergoing a strong self-propagating combustion reaction (SPCR) with the evolution of a large volume of gases. The entire combustion process was over within a few minutes yielding fine particles of γFe$_2$O$_3$. The products obtained employing the different weight ratios of α-Fe$_2$O$_3$: PEG mentioned above were named VH$_2$, VH$_3$, VH$_4$ and VH$_5$, respectively and pure α-Fe$_2$O$_3$ named as VH$_1$. From earlier studies (Venkataraman *et al* 2001; Vijay and Venkataraman 2001), it was found and reported that monophasic γFe$_2$O$_3$ was formed, when the ratio of α-Fe$_2$O$_3$: PEG was 1 : 5. Hence, the sample VH$_5$ represents pure and monophasic γFe$_2$O$_3$ and the other samples are found to have mixed phases of α-Fe$_2$O$_3$ and γFe$_2$O$_3$.

3. Characterization

3.1 Dielectric measurements

The experimental set up to measure dielectric properties of ferrites consist of a capacitance bridge (General Radio Type 1615A) with a three terminal network and a crystal holder assembly. The crystal holder assembly was provided with steel electrodes each having diameter of 1 cm. The test specimens used for the determination of dielectric constant were in the form of discs of thickness 0·28 cm and diameter of 1 cm. The specimens were painted with conducting silver paint for providing good electrical contact and were clamped firmly between the electrodes. The arrangement was found to provide good ohmic contact between the sample and the electrodes.

3.2 Infrared spectroscopy

The Fourier transform infrared spectroscopy (FTIR) of the samples were recorded on Nicolet-360 FTIR spectrometer using KBr pellet.

3.3 Electrical conductivity

Measurement of d.c. electrical conductivity, σ (mho·cm^{-1}), and its variation with temperature was carried out using a two-probe method over a temperature range 40–700°C. The sample holder consisted of two stainless steel elec-

trodes, each having a thickness of 2 cm and an area of 3 sq. cm. A Kanthol wire wounded on vertical muffle furnace, which can go up to 1000°C was used to study temperature variation of electrical conductivity by the sample. A d.c. voltage of 1·5 V was passed through the sample and the corresponding current was measured with the help of an electrometer (Keithley model No. 614). A calibrated chromel–alumel thermocouple was used to measure the temperature of the specimen. The samples of 0·28 cm in thickness and 1 cm in diameter were employed for this study. The specimens were painted with conducting silver paint for providing good electrical contact and were clamped firmly between the electrodes for measurement.

4. Results and discussion

4.1 Dielectric behaviour

The variation of dielectric constant (ε) with frequency at room temperature for all the samples VH$_1$ to VH$_5$ under investigation has been shown in figure 1 (a–e). It was observed from these figures that the dielectric constant decreases continuously with increase in frequency for all the samples, followed with a frequency independent behaviour. All samples show a dielectric constant of 25–30 at 10 kHz and a decreasing trend is observed at higher frequencies. This is a normal behaviour for high density, fine chemically homogeneous ferrimagnetic material (Katsumi *et al* 1975). The dielectric properties of ferrites are dependent upon several factors, including the method of preparation, chemical composition and grain structure and size (Murthy 1990). This may be explained qualitatively by the fact that electronic exchange between ferrous and ferric ions cannot follow the frequency of externally applied alternating field beyond a critical frequency value (Iwauchi 1971). The observed dielectric behaviour of our samples may also be due to the particle size effect and is also in concurrence with observation made by other investigators (Das and Pramanik 1998; Rane *et al* 2001). The effect of temperature on γFe$_2$O$_3$ sample (sample VH$_5$) is studied. Figure 2 shows the behaviour of dielectric constant with temperature at a constant frequency of 100 kHz. It is observed that, the dielectric constant value of the sample at 18 slowly increases up to 300°C, showing almost a temperature independent behaviour. It is understood that the dielectric constant (ε) and relaxation frequency, f_D, are related and depend on temperature (Abdeen 1999). If ε remains unaffected with increase in temperature then f_D also remains the same, that means that the local carriers are immobile. From figure 2, it is understood that the local charge carriers are immobile and the thermal activation is negligible. This further suggests that the sample VH$_5$ possesses a high chemical homogeneity and fine grain distribution.

4.2 Infrared spectroscopy

Infrared spectroscopic studies were performed aiming to ascertain the metal oxygen nature of the product and to follow the dehydration process. The FTIR of the samples VH_1 to VH_5 are shown in figure 3 (a–e). Sample VH1 showed the absorption in the region 3419, 1624, 1400, 546 and 458 cm^{-1}. The general range of 3600–3100 cm^{-1} (relating to antisymmetric and symmetric OH stretching) may be assigned for water of hydration. Hydrates also absorb in the region 1670–1600 cm^{-1} (relating to OH bending) (Miller and Wilkins 1952). This latter bond can be taken as another important means of identifying water of crystallization and it has been found very useful in the elucidation of crystal structure. In sample VH_1 (figure 3a), the band associated with the lattice water molecule is broad, and observed in a region of 3418 and 1624 cm^{-1}. The simultaneous presence of these two bands at 3418 and 1624 cm^{-1} indicates that, the water of crystallization is likely in the sample. The presence of water is also indicated by the electrical conductivity results. It is reported that presence of water plays an important role in the formation and stabilization of **g**Fe₂O₃ (Chopra *et al* 1999; Bourlions *et al* 2002; Rahman and Venkataraman 2002). The bands at 545·9 and 458 cm^{-1} are also observed in the sample, which are due to the metal oxygen stretching vibrational modes. These two bands are sharp and are of
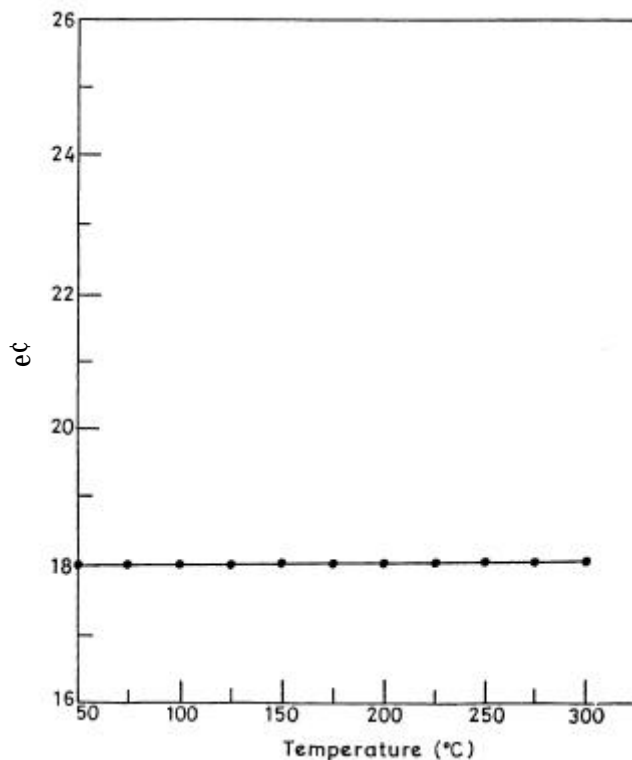
Figure 2. Dielectric constant with temperature behaviour at 100 kHz for VH₅ sample.
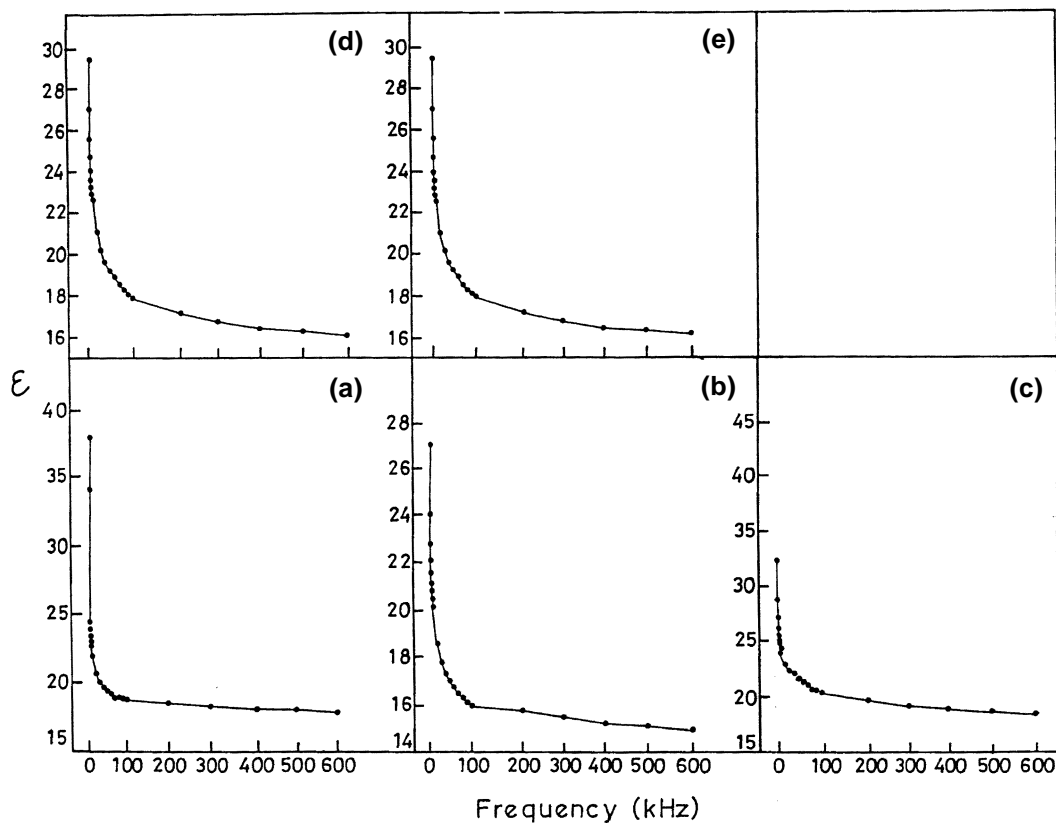
Figure 1. Dielectric behaviour of VH samples: (**a**) VH₁, (**b**) VH₂, (**c**) VH₃, (**d**) VH₄ and (**e**) VH₅.

strong intensity. The position of these two bands depends on the history of the sample. The sample VH_2 (figure 3b) showed peaks at 3458, 1679, 1107, 555·5 and 453·32 cm^{-1}. The peak at 3418 cm^{-1} of sample VH_1 shifted to 3458 cm^{-1} for sample VH_2. Also the peaks at 1624 cm^{-1} shifted to 1679 cm^{-1} and 545·5 to 555·5 cm^{-1} when compared with VH1 sample. All the peaks shifted to a higher region. This is due to the absorbed O_2 and some amount of H_2O being removed from $\mathbf{g}Fe_2O_3$ which is also observed from the electrical conductivity study discussed below. The weak peak at 1107 cm^{-1} may be due to some overtones. The infrared spectra of samples VH_3 and VH_4 (figures 3c and d) show the same behaviour as that observed for sample VH_2, but the intensity of the broad peaks at 3600–3000 cm^{-1} is found to be decreasing from VH_2 to VH_4 samples. Sample VH_5 i.e. pure $\mathbf{g}Fe_2O_3$ (figure 3e), showed the adsorption band around 3450, 1630, 546 and 458 cm^{-1}. The effect of particle size on infrared spectra has already been reported (Coey 1972). The shifts observed for the above samples may possibly be due to the particle size effect, as these samples have particle sizes of 0·1 to 10 μm.

4.3 *Electrical conductivity*

The variation of electrical conductivity, $\mathbf{s}$ (mho, cm^{-1}), with temperature was determined under static air for the samples VH_1 to VH_5, and is shown in figure 4 (a–e). Figure 4a for sample VH_1 shows that, $\mathbf{s}$, initially increases up to 140°C and then it decreases on further heating up to a temperature of 180°C. Thereafter, $\mathbf{s}$, increases rather slowly but linearly following an Arrhenius behaviour up to 800°C. The initial rise and later decrease in $\mathbf{s}$, in the region 140–180°C is due to the desorption of some absorbed water molecules. The observation of the peak in the region for desorption of absorbed water is in agreement with the earlier results (Venkataraman and Mukhedkar 1988; Rahman and Venkataraman 2002). Figure 4b for sample VH_2 shows that the $\mathbf{s}$ does not change much with variation of temperature from 60–140°C. On further increase in temperature the value of $\mathbf{s}$ increases showing a kink at 180°C and later a steep increase in $\mathbf{s}$ is observed from 180 to 340°C, and on further heating it remains constant up to 440°C, and thereafter it rises sharply. The region of plateau (340–440°C), which is also called a constant, $\mathbf{s}$, region may be assigned to the $\mathbf{g}Fe_2O_3 \rightarrow \mathbf{a}$-$Fe_2O_3$ phase transformation region. The observation of this plateau is similar to the $\mathbf{g} \rightarrow \mathbf{a}$ transformation as explained by other workers (Kawasaki and Miinowa 1966; Venkataraman and Mukhedkar 1988). The presence of kink at 180°C indicates the possibility of a hydrogen ferrite phase at this temperature and that the hydrogen ferrite phase decomposes to give a purely vacancy ordered $\mathbf{g}$
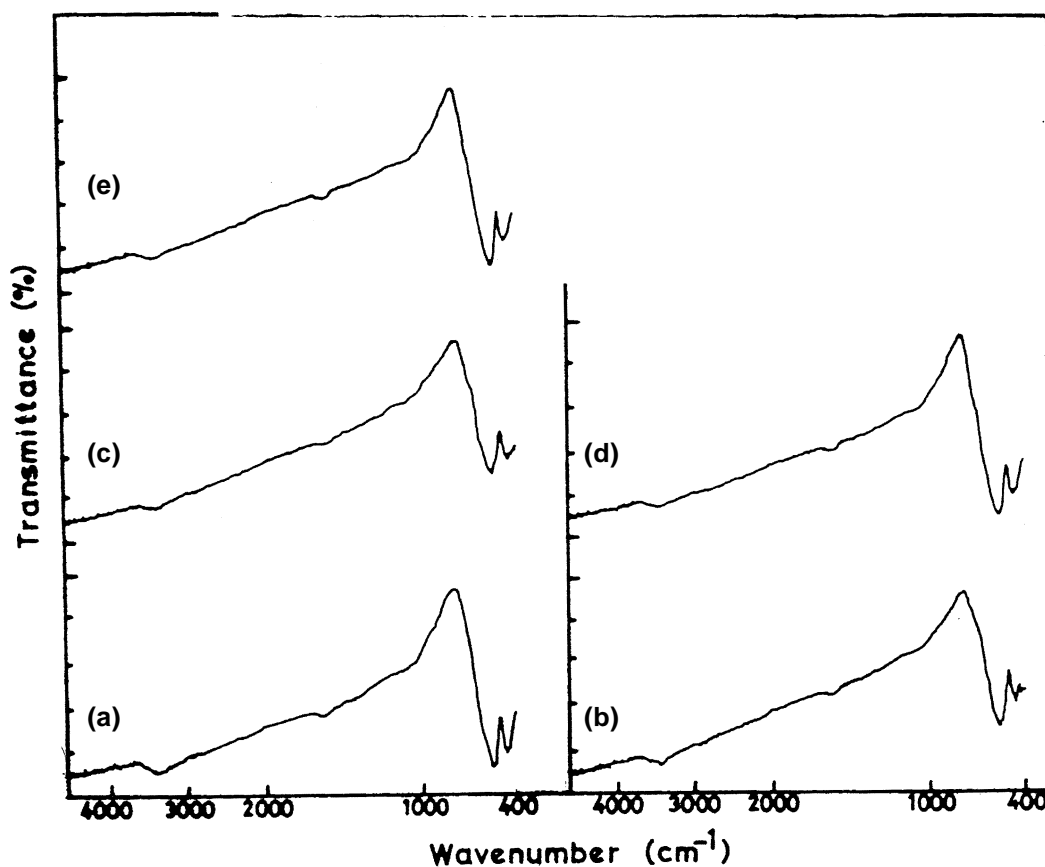

Figure 3. The FTIR spectra of VH samples: (**a**) VH_1, (**b**) VH_2, (**c**) VH_3, (**d**) VH_4 and (**e**) VH_5.
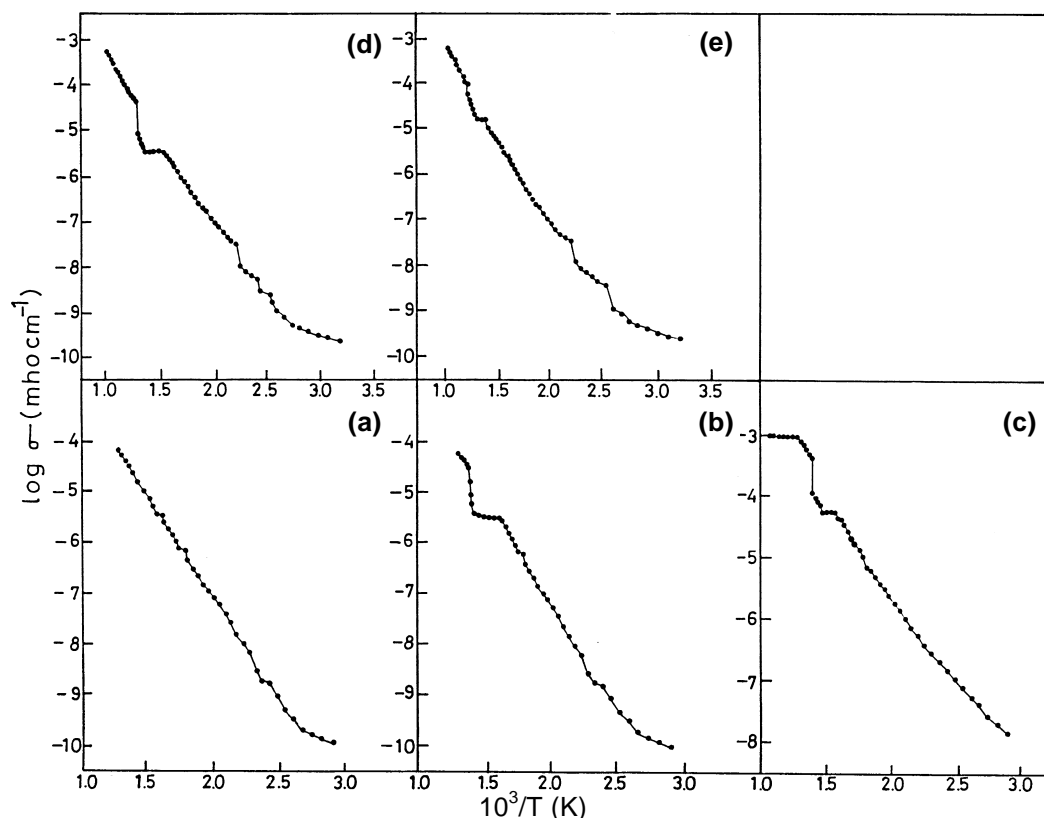
Figure 4. Electrical conductivity vs temperature behaviour for VH samples: (**a**) VH₁, (**b**) VH₂, (**c**) VH₃, (**d**) VH₄ and (**e**) VH₅.

Fe_2O_3 which was observed from the X-ray pattern. In sample VH₃, it is observed that the plot of log **s** against T^{-1} shows a small kink at 270–310°C. This kink is similar to that observed for ≤ **g**Fe₂O₃ synthesized from ferrous carboxylates (Venkataraman and Mukhedkar 1988). This small kink observed is due to the decomposition of hydrogen ferrite phase in VH₃ sample. On further rise in the temperature, there is a slow transformation of **g**Fe₂O₃ to **a**-Fe₂O₃ in a temperature range of 370–430°C, which is indicated with the presence of a plateau.

The plot of log **s** against T^{-1} for the samples VH₄ and VH₅ observed in figure 4 (d and e) shows similar behaviour. It is observed that, as the temperature is increased, there is an increase in **s** value up to 120°C. On further rise in temperature it shows a kink in the region of 120 to 180°C indicating that, at this temperature, the hydrogen ferrite phase is decomposed as explained earlier. The steep of **s** in the temperature range of 180–360°C indicates the formation of pure vacancy ordered **g**Fe₂O₃. On further rise in temperature there is a slow transformation of **g** Fe₂O₃ → **a**-Fe₂O₃. However, the temperature region of this phase transition is different in sample VH₄ (figure 4d), the region is from 360–510°C. It can be noted that as the amount of polyethylene glycol (as fuel) is increased the phase transformation of **g**Fe₂O₃ → **a**-Fe₂O₃ also increased. The observed electrical conductivity results indicate

that **g**Fe₂O₃ samples have only Fe^{+3} state in tetrahedral and octahedral positions. The change in **s** is due to the particle size effect. The particle size and shape were found to be different for the VH series. Hence, it may be understood here that the particle morphology also plays an important role in the shifting of the temperature region for the transition.

5. Conclusions

The effect of chemical homogeneity, fine grain structure, particle size and shape of the ferrite samples are understood to affect the properties viz. dielectric, electrical conductivity and infrared spectral studies. The presence of **a**-impurities also contribute towards changes in these properties.

References

Abdeen A M 1999 *J. Magn. Magn. Mater.* **192** 121

Aruna S T, Gosh S and Patil K C 2001 *Int. J. Inorg. Mater.* **3** 387

Bourlions A B, Simopoulos A and Petridos D 2002 *Chem. Mater.* **14** 889

Chopra G S, Real C, Alcala M D, Perez Maqueda L A, Subrt J and Carido J M 1999 *Chem. Mater.* **11** 1128

Coey J M D 1972 *J. Phys. Status Solidi* (a)**11** 229

Das R N and Pramanik P 1998 *Nanostruct. Mater.* **10** 1371

Eberhard K and Thomas C A 1998 *Magnetic recording hand book*, *technology and applications* (eds) M C Denis and D D Eric (New York: McGraw Hill Co.) Ch. 3, p. 101

Gopal Reddy G V, Kalyana Sheela and Manorama S V 2000 *Int. J. Inorg. Mater.* **2** 301

Gulabshankar R Dube and Darshane V S 1991 *Bull. Chem. Soc. Jpn* **64** 2449

Iwauchi Kozo 1971 *Jpn J. Appl. Phys.* **10** 1520

Jung K and Feldmann C 2000 *J. Mater. Res.* **15** 536

Katsumi K, Mamoru S, Tatsuo I and Katsuya I 1975 *Bull. Chem. Soc. Jpn* **48** 1764

Kawasaki T and Miinowa Z 1966 *J. Appl. Phys. Jpn* **35** 355

Mallikarjun N N 2002 *Synthesis, characterization and some studies of ferrites—Polymer composites*, Ph D Thesis, Gulbarga University, Gulbarga (submitted)

Mallikarjuna N N and Venkataraman A 2003 *Indian J. Engg. Mater. Sci.* **10** 50

Miller F A and Wilkins C H 1952 *J. Anal. Chem.* **24** 1253

Murthy V R K 1990 *Low frequency dielectric properties of ferrites* (eds) V R K Murthy and B Viswanatham (New Delhi: Narosa Publication) Ch. IV, ed. 1

Murthy V R K and Sobhanadri J 1976 *J. Phys. Status Solidi* **(a)36k** 133

Rahman M M and Venkataraman A 2002 *J. Therm. Anal. Cal.* **68** 91

Rane K S, Verenkar V M S and Sawant P Y 2001 *Bull. Mater. Sci.* **24** 323

Sale F R, Fan J and Chien Y T 1995 *Am. Ceram. Trans.* **47** 155

Venkataraman A, Vijay A Hiremath, Date S K and Kulkarni S D 2001 *Bull. Mater. Sci.* **24** 617

Venkataraman A and Mukhedkar A J 1988 *J. Mater. Sci.* **23** 3005

Vijay A Hiremath and Venkataraman A 2001 *Ind. Prod. Find. (India)* **29** 300

Waldron R D 1955 *Phys. Rev.* **99** 1721

Young S K, Subhash R, John F R and Pieter S 1996 *Chem. Mater.* **8** 2209